Absence of a quantum limit to charge diffusion in bad metals

Nandan Pakhira* and Ross H. McKenzie†

School of Mathematics and Physics, The University of Queensland, Brisbane QLD 4072, Australia

(Received 3 October 2014; revised manuscript received 23 January 2015; published 23 February 2015)

Good metals are characterized by diffusive transport of coherent quasiparticle states and the resistivity is much less than the Mott-Ioffe-Regel (MIR) limit, $\frac{ha}{e^2}$, where a is the lattice constant. In bad metals, such as many strongly correlated electron materials, the resistivity exceeds the Mott-Ioffe-Regel limit and the transport is incoherent in nature. Hartnoll, loosely motivated by holographic duality (AdS/CFT correspondence) in string theory, recently proposed a lower bound to the charge-diffusion constant, $D \gtrsim \hbar v_F^2/(k_B T)$, in the incoherent regime of transport, where v_F is the Fermi velocity and T the temperature. Using dynamical mean-field theory (DMFT) we calculate the charge-diffusion constant in a single band Hubbard model at half filling. We show that in the strongly correlated regime the Hartnoll's bound is violated in the crossover region between the coherent Fermi-liquid region and the incoherent (bad metal) local moment region. The violation occurs even when the bare Fermi velocity v_F is replaced by its low-temperature renormalized value v_F^*. The bound is satisfied at all temperatures in the weakly and moderately correlated systems as well as in strongly correlated systems in the high-temperature region where the resistivity is close to linear in temperature. Our calculated charge-diffusion constant, in the incoherent regime of transport, also strongly violates a proposed quantum limit of spin diffusion, $D_s \sim 1.3\hbar/m$, where m is the fermion mass, experimentally observed and theoretically calculated in a cold degenerate Fermi gas in the unitary limit of scattering.

DOI: 10.1103/PhysRevB.91.075124 PACS number(s): 71.27.+a, 05.60.Gg, 67.10.Jn

I. INTRODUCTION

Good metals like copper and gold are characterized by high optical reflectivity and electrical and thermal conductivity. The transport in these systems can be characterized by diffusive transport of coherent quasiparticle states, where the mean-free path is much larger than the lattice constant. The low-temperature resistivity in good metals is well within the Mott-Ioffe-Regel (MIR) limit, $\frac{ha}{e^2} \sim 250\ \mu\Omega\,\mathrm{cm}$, where a is the lattice constant. However, in a large class of strongly correlated systems like $3d$ transition metal oxide compounds and most notably in the strange metal regime of doped cuprates (high-T_c superconductors) at optimal doping the resistivity far exceeds the MIR limit [1] and hence cannot be characterized by diffusive transport of coherent quasiparticle states in the limit of weak scattering. Other signatures of a bad metal include a thermopower of order k_B/e, the absence of a Drude peak in the optical conductivity, and a nonmonotonic temperature dependence of the Hall constant and thermopower [2–4].

There have been a range of theoretical attempts to understand the incoherent regime of transport, especially for the strange metal phase of doped cuprates (high-T_c superconductors) at optimal doping. Recently, there is a string theory based approach to understand transport in the incoherent regime [5,6]. String theory, originally proposed as a possible theory for quantum gravity, is mathematically consistent but yet has no experimental verification. In the following paragraph we briefly describe how a string theory based approach has been proposed to describe transport in condensed-matter systems.

Maldacena conjectured [7] that the large-N limit of certain supersymmetric conformal field theory (CFT) has correspondence to supergravity in anti–de Sitter (AdS) spaces in higher dimension. This is known as the *AdS/CFT correspondence* or *gauge/gravity duality*. The most famous example of AdS/CFT correspondence states that IIB string theory in the product space $\mathrm{AdS}_5 \times S^5$ is dual to large N_c limit of $\mathcal{N} = 4$ supersymmetric $\mathrm{SU}(N_c)$ Yang-Mills theory on the four-dimensional boundary. Further AdS/CFT correspondences relate fluid dynamics to event horizon dynamics of a black hole in anti–de Sitter space. In the hydrodynamic regime (long-wavelength limit) of the correspondence, Einstein's equations of general relativity reduce to the Navier-Stokes equation for fluid mechanics. Classical fluids are characterized by transport coefficients such as shear viscosity and diffusion constant. Using the AdS/CFT correspondence Kovtun *et al.* [8] calculated the ratio, η/s, of the shear viscosity (η) and the entropy density (s) and proposed a lower bound $\frac{\eta}{s} \geqslant \frac{\hbar}{4\pi k_B}$. Such a bound is respected in classical fluids like water, the quark-gluon plasma (QGP) created in the relativistic heavy ion collider (RHIC) [9], and in experiments on cold degenerate Fermi gases in the unitary limit [10]. However, some violations of this bound have been reported [11]. Inspired by the bound on the viscosity and also using the AdS/CFT correspondence Hartnoll recently proposed [12] a lower bound for the diffusion constant,

$$D \gtrsim \mathcal{D}_H \equiv \frac{\hbar v_F^2}{k_B T}, \tag{1}$$

in the incoherent regime of transport in strongly correlated electron systems. But, except near quantum critical point, condensed-matter systems are probably neither relativistic nor conformal [13]. So, this proposal needs to be tested against model based calculations.

The temperature-dependent diffusion constant, $D(T)$, is related to the temperature-dependent conductivity, $\sigma(T)$, through the *Nernst-Einstein relation*

$$\sigma(T) = e^2 \frac{\partial n}{\partial \mu} D(T). \tag{2}$$

*npakhira@gmail.com
†r.mckenzie@uq.edu.au; condensedconcepts.blogspot.com

where $\kappa_e(T) = \frac{\partial n}{\partial \mu}$ is the *charge compressibility*. For completeness we give a derivation of this relation in the Appendix. Because of the above relation knowledge of the charge-diffusion constant $D(T)$ may help us to better understand the electrical conductivity $\sigma(T)$.

Experiments on cold degenerate Fermi gases in the unitary scattering limit show a quantum limit to the spin-diffusion constant [14,15], $D_s \simeq 1.3\hbar/m$. This bound is also supported by theoretical calculations [16]. However, experiments on a two-dimensional Fermi gas found a value D_s that was more than two orders of magnitude smaller than the proposed bound [17]. But spin diffusion in charge neutral systems such as cold atomic gases has no obvious relation to charge diffusion in charged quantum fluids such as strongly correlated electron systems. For example, in a Mott insulator the charge-diffusion constant is zero but the spin-diffusion constant is nonzero. Hence, it is conceivable that in a bad metallic phase close to the Mott insulator the charge-diffusion constant is much smaller than the spin-diffusion constant. In the present paper we do a model based calculation of the charge-diffusion constant in a Hubbard model, and explore the possible existence of a lower bound to the charge-diffusion constant and its possible relation to spin diffusion in atomic gases.

The organization of the paper is as follows. In Sec. II we introduce the single band Hubbard model and its solution under single-site dynamical mean-field theory (DMFT). We also briefly describe DMFT self-consistency using iterated perturbation theory (IPT) as a solver for the impurity problem arising under single-site DMFT. In Sec. III we briefly introduce calculation of transport and thermodynamic quantities under the single-site DMFT approximation. Then in Sec. IV we show our results for a single band Hubbard model on the Bethe lattice at half filling. We find clear violation of Hartnoll's proposed bound, even when the bare Fermi velocity v_F is replaced by the low-temperature renormalized velocity, v_F^*. Finally, in Sec. V we conclude and briefly consider how relaxing some of our assumptions may modify the results.

II. MODEL BASED CALCULATIONS

We consider the single band Hubbard model with nearest-neighbor hopping, described by the Hamiltonian

$$H = -t \sum_{\langle i,j\rangle,\sigma} (c_{i\sigma}^\dagger c_{j\sigma} + \text{H.c.}) - \mu \sum_{i,\sigma} n_{i\sigma} + U \sum_i n_{i\uparrow} n_{i\downarrow}, \quad (3)$$

where $n_{i\sigma} = c_{i\sigma}^\dagger c_{i\sigma}$, t is the hopping amplitude, μ is the chemical potential, and U is the Coulomb repulsion for a doubly occupied site. This is probably the simplest model which incorporates nontrivial strong correlation effects. But this model has an exact solution only in one dimension and study of this model in higher dimensions involves various approximations. Static mean-field descriptions like the Hartree-Fock decomposition of the quartic term $Un_{i\uparrow}n_{i\downarrow} \simeq U\langle n_{i\uparrow}\rangle n_{i\downarrow} + Un_{i\uparrow}\langle n_{i\downarrow}\rangle$ only shifts the local chemical potential. Because of the complete neglect of the quantum fluctuations this approximation does not generate any new energy scale (e.g., the Fermi-liquid coherence scale) which can become relevant at low-temperature regions. However, as in the case of classical mean-field theory for the Ising model, in the limit of large dimension, $d \to \infty$ (or large connectivity z) the model reduces to an effective single impurity model provided the scaling $t \to t^*/\sqrt{2d}$ is made on a d-dimensional hypercubic lattice [18]. Under this approximation we neglect all spatial fluctuations yet fully retain quantum dynamics for the single site. The self-energy $\Sigma(\omega)$ only depends on frequency and not wave vector. This is known as the dynamical mean-field theory [19] (DMFT). It has been found that DMFT gives a good description of the Mott metal-insulator transition with increasing correlation strength U and the crossover from a Fermi liquid to bad metal with increasing temperature [2]. Furthermore, DMFT has been found to give a quantitative description of the temperature dependence of the resistivity [20] and the frequency dependent optical conductivity [21] for organic charge-transfer salts that are described by a two-dimensional Hubbard model at half filling [22]. Combining DMFT with electronic structure calculations based on density functional theory has given an excellent description of properties of a diverse range of transition metal and rare earth compounds [23].

A. Dynamical mean-field theory

As a consequence of the scaling, $t \to t^*/\sqrt{2d}$, all the self-energy diagrams, arising under skeletal graph expansion of the irreducible self-energy and involving nonlocal Green's functions, vanish in the limit $d \to \infty$. Then the self-energy becomes local and involves only the local Green's function. The lattice problem for the Hubbard model then can be mapped onto an effective single impurity Anderson model [19]:

$$H_{\text{imp}} = \sum_{l,\sigma} (\tilde{\epsilon}_l - \mu) c_{l\sigma}^\dagger c_{l\sigma} + \sum_{l,\sigma} (V_l c_{l\sigma}^\dagger d_{0\sigma} + \text{H.c.}) - \mu \sum_\sigma n_{d0\sigma} + U n_{d0\uparrow} n_{d0\downarrow}, \quad (4)$$

where $n_{d0\sigma} = d_{0\sigma}^\dagger d_{0\sigma}$. The operators $d_{0\sigma}^\dagger$ and $d_{0\sigma}$ characterize a given site $i = 0$ and $\{c_{l\sigma}^\dagger, c_{l\sigma}\}$ characterize the effective bath arising from electrons at all other sites. $\tilde{\epsilon}_l$ and V_l are effective parameters characterizing the dispersion of the bath and its coupling to the local site. $\tilde{\epsilon}_l$ and V_l or equivalently the bath Green's function, given by $G_0(\omega)$,

$$G_0^{-1}(\omega) = \omega + \mu - \int_{-\infty}^{+\infty} \frac{\Delta(\epsilon)\, d\epsilon}{\omega + \mu - \epsilon},$$
$$\Delta(\epsilon) = \sum_{l\sigma} V_l^2 \delta(\epsilon - \tilde{\epsilon}_l), \quad (5)$$

can be calculated self-consistently by solving the impurity problem iteratively. The solution of the impurity problem is the toughest part and usually involves use of numerical methods such as quantum Monte Carlo (QMC), exact diagonalization (ED), or the numerical renormalization group (NRG).

We use iterated perturbation theory (IPT) [24,25] as it is easy to implement, computationally cheap, and captures the essential physics in the parameter regime we are interested in, $U < 0.8U_c$ where U_c is the critical value of U at which the Mott metal-insulator transition occurs. For example, Bulla [26] showed that for the Bethe lattice at half filling the results of IPT and NRG are similar except extremely close to the Mott

transition. Indeed in the proximity of the Mott transition, Terletska *et al.* [27] found that the temperature-dependent resistivity calculated from IPT was in agreement with that found by continuous time QMC (CT-QMC). Also, recently Arsenault *et al.* [28] showed that for lattices with a van Hove singularity in the density of states (DOS), even in the proximity of the Mott transition IPT with a modified self-consistency condition matches results from CT-QMC. So, for the single band Hubbard model results from the IPT are generic in nature. In the next section we review DMFT self-consistency using IPT.

B. Iterated perturbation theory

The iterated perturbation theory (IPT) is a semianalytical method. The irreducible self-energy in IPT is approximated using a second-order polarization bubble involving the bath Green's function, $G_0(\omega)$. The self-energy under this approximation can be shown (using moment expansion) to smoothly interpolate between the atomic limit $t = 0$ and the weak-coupling limit $U \to 0$. In the following paragraph we elaborate on the DMFT self-consistency method using IPT as the impurity solver. We work with real, not imaginary, frequencies and so no analytic continuation is necessary.

(i) For a given lattice density of states $N_0(\epsilon)$ and self-energy $\Sigma(\omega)$ the *local* Green's function is given by

$$G(\omega) = \int_{-\infty}^{+\infty} \frac{N_0(\epsilon)d\epsilon}{\omega^+ + \mu - \Sigma(\omega^+) - \epsilon}, \tag{6}$$

where μ is the *local* chemical potential.

(ii) From knowledge of the *local* Green's function $G_{\rm loc}(\omega)$ we can calculate the *bath hybridization* function $\Delta(\omega)$ by using

$$\Delta(\omega) = \omega^+ + \mu - \Sigma(\omega) - G^{-1}(\omega). \tag{7}$$

(iii) Subsequently using *bath hybridization* we can calculate the *bath Green's function* as

$$G_0(\omega) = \frac{1}{\omega + \tilde{\mu}_0 - \Delta(\omega)}. \tag{8}$$

The parameter $\tilde{\mu}_0 = \mu - Un$ is the bath chemical potential and it vanishes at half filling for the particle-hole symmetric case, which we consider in the present study.

(iv) The fully interacting Green's function can be calculated using the Dyson's equation

$$G(\omega) = \frac{1}{G_0^{-1}(\omega) - \tilde{\mu}_0 + \mu - \Sigma(\omega)}. \tag{9}$$

(v) The new self-energy can be calculated following the IPT ansatz [25] as

$$\Sigma(\omega) = Un + \frac{A\Sigma^{(2)}(\omega)}{1 - B\Sigma^{(2)}(\omega)}, \tag{10}$$

where

$$A = \frac{n(1-n)}{n_0(1-n_0)}; \quad B = \frac{U(1-n) - \mu + \mu_0}{n_0(1-n_0)U^2} \tag{11}$$

and

$$n = -\frac{1}{\pi}\int_{-\infty}^{+\infty} d\omega\, n_F(\omega)\, \mathrm{Im}[G(\omega^+)], \tag{12}$$

$$n_0 = -\frac{1}{\pi}\int_{-\infty}^{+\infty} d\omega\, n_F(\omega)\, \mathrm{Im}[G_0(\omega^+)] \tag{13}$$

are the *local* and *bath* particle numbers, respectively. $\Sigma^{(2)}(\omega)$ is the self-energy from second-order perturbation theory and is given by

$$\Sigma^{(2)}(\omega) = U^2 \int_{-\infty}^{+\infty} \prod_{i=1}^{3} [d\epsilon_i \rho_0(\epsilon_i)] \left[\frac{n_F(-\epsilon_1) n_F(\epsilon_2) n_F(-\epsilon_3)}{\omega + i\eta - \epsilon_1 + \epsilon_2 - \epsilon_3} + \frac{n_F(\epsilon_1) n_F(-\epsilon_2) n_F(\epsilon_3)}{\omega + i\eta - \epsilon_1 + \epsilon_2 - \epsilon_3} \right], \tag{14}$$

where $\rho_0(\omega) = -\frac{1}{\pi}\mathrm{Im}[G_0(\omega^+)]$ and $\eta \to 0^+$. We iterate (i)–(v) until the desired self-consistency in self-energy and other physical quantities are achieved. Hence, we focus solely on the case of half filling ($n = 1$). Due to particle-hole symmetry $\mu = \frac{U}{2}$ for all U and T. This speeds up computation significantly, as it is not necessary to self-consistently determine μ from Eq. (12).

C. Bethe lattice

We choose a Bethe lattice (Cayley tree) because it makes computation even faster because the local Green's function $G(\omega)$ has an exact analytical form. Particle-hole symmetry also simplifies the calculations. The Bethe lattice produces qualitatively similar results to the hypercubic lattice [19] and lower dimensional Hubbard models [4,21]. In the limit of infinite coordination number ($z \to \infty$), the density of states has *semicircular* form [29]:

$$N_0(\epsilon) = \frac{2}{\pi W^2}\sqrt{W^2 - \epsilon^2}\, \Theta(W - |\epsilon|), \tag{15}$$

where $\Theta(x)$ is the familiar unit step function, $W = 2t^*$ is the half bandwidth and the hopping amplitude in this case is scaled as $t \to t^*/\sqrt{z}$. Most importantly the *local* Green's function has the exact analytical form

$$G(\omega) = \frac{2}{W^2}[\zeta - \sqrt{\zeta^2 - W^2}], \tag{16}$$

$$\zeta(\omega) \equiv \omega + i\eta + \mu - \Sigma(\omega). \tag{17}$$

It can be easily verified that in this case the *bath hybridization* function, $\Delta(\omega) = \frac{W^2}{4}G(\omega) \equiv t^{*2}G(\omega)$, is proportional to the *local* Green's function.

III. TRANSPORT PROPERTIES

Using the self-consistent self-energy we can calculate various quantities like dc conductivity, charge compressibility, and diffusivity.

A. dc conductivity

In the limit of $d \to \infty$ all vertex corrections to two-body correlation functions drop out [30] and the temperature-dependent dc conductivity, $\sigma(T)$, can be calculated using the

simple polarization bubble as [19,31]

$$\sigma(T) = \frac{\pi e^2}{\hbar}\frac{1}{v}\int_{-\infty}^{+\infty} d\epsilon\ \Phi_{xx}(\epsilon) \times \int_{-\infty}^{+\infty} d\omega\left(-\frac{\partial n_F(\omega)}{\partial\omega}\right)A^2(\omega,\epsilon), \quad (18)$$

where $v = a^d$ is the volume of the unit cell of a d-dimensional hypercubic lattice with lattice constant a,

$$A(\omega,\epsilon) = -\frac{1}{\pi}\mathrm{Im}\left[\frac{1}{\omega+\mu-\Sigma(\omega)-\epsilon}\right], \quad (19)$$

$$n_F(\omega) = \frac{1}{e^{\beta\omega}+1} \quad (20)$$

are the spectral density and Fermi function, respectively, and

$$\Phi_{xx}(\epsilon) = \frac{1}{N}\sum_{\mathbf{k}}\left(\frac{\partial\epsilon_{\mathbf{k}}}{\partial k_x}\right)^2\delta(\epsilon-\epsilon_{\mathbf{k}}) \quad (21)$$

is the *transport density of states*. N is the number of lattice sites.

Because of its treelike structure the Bethe lattice has no loop and no energy dispersion relation in $\mathbf{k}$. But, by invoking the f-sum rule it can be shown that [32–34]

$$\Phi_{xx}(\epsilon) = \frac{1}{3d}(W^2-\epsilon^2)N_0(\epsilon) \quad (22)$$

is the correct *transport density of states* in the limit of $d\to\infty$. It is interesting to mention that for a Bethe lattice with coordination number z the connectivity $K = z-1$ while that for the hypercubic lattice is $2d$. So, in the limit of large coordination number we can take the connectivity to be equal to $2d$ and we can always do the mapping $z \leftrightarrow 2d$.

B. Charge compressibility

The inverse of the charge compressibility can be interpreted as the energy cost to add or remove a particle from a system. For the noninteracting system ($U = 0$) at zero temperature ($T = 0$), $\kappa_e = N_0(E_F)$, where $N_0(E_F)$ is the density of states at the Fermi level.

In a general many-body system the local particle number is given by

$$n = \frac{1}{v}\int_{-\infty}^{+\infty} d\omega\, n_F(\omega)\sum_{\mathbf{k}} A(\mathbf{k},\omega), \quad (23)$$

where the spectral function is

$$A(\mathbf{k},\omega) = -\frac{1}{\pi}\mathrm{Im}\left[\frac{1}{\omega+\mu-\epsilon_{\mathbf{k}}-\Sigma_{\mathbf{k}}(\omega)}\right]. \quad (24)$$

The self-energy, $\Sigma_{\mathbf{k}}(\omega)$, in the limit of $d\to\infty$ is independent of wave vector $\mathbf{k}$ and is given by $\Sigma(\omega)$. Hence, differentiating with respect to μ, the charge compressibility, $\kappa_e(T) = \frac{\partial n}{\partial\mu}$, under the DMFT approximation is given by

$$\kappa_e(T) = \frac{1}{\pi}\mathrm{Im}\int_{-\infty}^{+\infty} d\omega\, n_F(\omega)\left(1-\frac{\partial\Sigma(\omega)}{\partial\mu}\right) \times \int_{-\infty}^{+\infty}\frac{N_0(\epsilon)\,d\epsilon}{[\omega+\mu-\Sigma(\omega)-\epsilon]^2}. \quad (25)$$

The effect of the derivative $\frac{\partial\Sigma(\omega)}{\partial\mu}$ on the charge compressibility of a Fermi liquid was discussed previously by Luttinger [35] and by Hotta and Fujimoto [36]. Here it does not have a closed analytical form and we evaluate it beginning with the IPT expression (10). The charge compressibility $\kappa_e(T)$ is then given by

$$\kappa_e(T) = \frac{\tilde{J}+\tilde{K}}{1+U(\tilde{J}+\tilde{K})}, \quad (26)$$

where the $\tilde{J}$ term in the denominator is associated with the Hartree term in the self-energy (10). For the Bethe lattice

$$\tilde{J} = -\frac{1}{\pi}\mathrm{Im}\int_{-\infty}^{+\infty} d\omega\, n_F(\omega)\left[2-\frac{2\zeta}{\sqrt{\zeta^2-1}}\right], \quad (27)$$

$$\tilde{K} = \frac{1}{\pi}\mathrm{Im}\int_{-\infty}^{+\infty} d\omega\, n_F(\omega)\left[2-\frac{2\zeta}{\sqrt{\zeta^2-1}}\right]\frac{\partial\tilde{\Sigma}_2(\omega)}{\partial\mu}, \quad (28)$$

and $\zeta(\omega)$ is given by Eq. (17). If we define $\frac{\partial\rho_\Sigma(\omega)}{\partial\mu} = -\frac{1}{\pi}\mathrm{Im}\frac{\partial\tilde{\Sigma}_2(\omega)}{\partial\mu}$ then

$$\frac{\partial\rho_\Sigma(\omega)}{\partial\mu} = \int d\epsilon_1 d\epsilon_2\left[2\frac{\partial\rho_{\mathcal{G}}(\epsilon_1)}{\partial\mu}\rho_{\mathcal{G}}(\omega-\epsilon_1+\epsilon_2)\rho_{\mathcal{G}}(\epsilon_2) + \rho_{\mathcal{G}}(\epsilon_1)\rho_{\mathcal{G}}(\omega-\epsilon_1+\epsilon_2)\frac{\partial\rho_{\mathcal{G}}(\epsilon_2)}{\partial\mu}\right] \times[n_F(-\epsilon_1)n_F(-\omega+\epsilon_1-\epsilon_2)n_F(\epsilon_2) + n_F(\epsilon_1)n_F(\omega-\epsilon_1+\epsilon_2)n_F(-\epsilon_2)], \quad (29)$$

where $\rho_{\mathcal{G}}(\omega) = -\frac{1}{\pi}\mathrm{Im}G_0(\omega)$ and for the Bethe lattice

$$\frac{\partial\rho_{\mathcal{G}}(\omega)}{\partial\mu} = -\frac{1}{\pi}\mathrm{Im}\frac{2-\frac{2\zeta}{\sqrt{\zeta^2-1}}}{4[\omega+\mu_0-\Delta(\omega)]^2}. \quad (30)$$

The expression in Eq. (29) is calculated by using the standard FFT routine and the real part of $\frac{\partial\tilde{\Sigma}_2(\omega)}{\partial\mu}$ can be calculated using Hilbert transform. We note in passing that we find for most parameter regimes that the expression (26) is dominated by the $\tilde{J}$ terms and the $\tilde{K}$ terms involve only a small correction.

C. Diffusivity

As mentioned earlier the diffusivity, $D(T)$ can be calculated using the *Nernst-Einstein relation* in Eq. (2). To compare to the limit of diffusion constant, proposed by Hartnoll, we need to find the Fermi velocity v_F. First, one has to decide whether this should be the bare Fermi velocity, i.e., the "band structure" value, or a renormalized value v_F^* associated with a low-temperature Fermi-liquid state. In that case, $v_F^* = Zv_F$ where Z is the quasiparticle renormalization factor which can be calculated from the self-energy, $\Sigma(\omega) = \Sigma_R(\omega) + i\Sigma_I(\omega)$:

$$Z = \left(1-\left.\frac{\partial\Sigma_R(\omega)}{\partial\omega}\right|_{\omega\to0}\right)^{-1}. \quad (31)$$

The Hartnoll bound $\mathcal{D}_H$ then gets renormalized to $\mathcal{D}_H^* = Z^2\mathcal{D}_H$. Note that as the Mott transition is approached this decreases the lower bound by several orders of magnitude, making it harder to violate. It is not completely clear to us from the arguments of Hartnoll whether one should use v_F or

v_F^*, particularly as he is concerned with incoherent transport, i.e., outside the Fermi-liquid regime. Here, we use the latter but note that this choice makes the bound much less stringent.

Second, there is the issue of how to evaluate the Fermi velocity in the DMFT approximation, in the limit of infinite dimensionality, $d \to \infty$. Since $v_{\mathbf{k}}^2 = (\frac{\partial \epsilon_{\mathbf{k}}}{\partial \mathbf{k}})^2$ appears in the expression for *transport density of states* in Eq. (21) we define

$$\hbar v_F^2 = \frac{1}{\hbar} \frac{\Phi_{xx}(\epsilon = 0)}{N_0(\epsilon = 0)} \tag{32}$$

in the limit of $d \to \infty$. This definition of $\hbar v_F^2$ gives the correct Fermi velocity [31] for the hypercubic lattice in the limit of $d \to \infty$. Also, by pure dimensional analysis for any lattice structure $\hbar v_F = \lambda W a$ (λ being a numerical constant of order 1 for a given lattice). Hartnoll's proposed quantum bound for diffusion constant on the Bethe lattice is then given by

$$\mathcal{D}_H = \frac{W^2 a^2}{3 d \hbar k_B T}. \tag{33}$$

Including the renormalization of the Fermi velocity the dimensionless scaled diffusivity is then given by

$$\frac{D(T)}{\mathcal{D}_H^*} = \pi \left(\frac{k_B T}{W}\right) \frac{1}{Z^2 \tilde{\kappa}_e(T)} \int_{-W}^{+W} d\epsilon \int_{-\infty}^{+\infty} d\omega (W^2 - \epsilon^2) \times N(\epsilon) A^2(\epsilon, \omega) \left(-\frac{\partial n_F(\omega)}{\partial \omega}\right), \tag{34}$$

where $\tilde{\kappa}_e(T) = \frac{\partial \tilde{n}}{\partial \tilde{\mu}}$ is the dimensionless charge compressibility and $\mu = \tilde{\mu} W$, $\tilde{n} = n v$. The advantage of calculating scaled diffusivity is that it does not depend on universal constants such as $\hbar$ or material dependent constants such as the lattice constant a and the unit cell volume v, and the temperature appears only as a dimensionless scaled quantity.

We now turn to comparison with the proposed bound for the spin-diffusion constant. In a similar spirit we use $\frac{1}{m} = \frac{1}{\hbar^2} \frac{\partial^2 \epsilon_{\mathbf{k}}}{\partial k_x^2}$ as a generalized definition for inverse mass. Then for the hypercubic lattice we get $\frac{W a^2}{d \hbar^2}$ as an effective inverse mass averaged over the Fermi surface at half filling. If we take this to be same in the Bethe lattice as well then we will have

$$\mathcal{D}_A = \frac{\alpha W a^2}{d \hbar} \tag{35}$$

with $\alpha = 1.3$ a dimensionless constant.

In an interacting system the bare mass m gets renormalized to an effective mass $m^* = m/Z$ where Z is the quasiparticle weight. Thus the bound $\mathcal{D}_A$ will get renormalized to

$$\mathcal{D}_A^* = \alpha \frac{\hbar}{m^*} = Z \mathcal{D}_A. \tag{36}$$

The scaled diffusivity in this case is then given by

$$\frac{D(T)}{\mathcal{D}_A^*} = \frac{\pi}{3 \alpha Z} \frac{1}{\tilde{\kappa}_e(T)} \int_{-W}^{+W} d\epsilon \int_{-\infty}^{+\infty} d\omega (W^2 - \epsilon^2) N(\epsilon) \times A^2(\epsilon, \omega) \left(-\frac{\partial n_F(\omega)}{\partial \omega}\right). \tag{37}$$

IV. RESULTS

We consider the case of half filling, $n = 1$, i.e., each site on the average is occupied by one electron. We study spectral and transport properties as a function of correlation strength U and temperature T (enters as $k_B T$ with dimension of energy). Henceforth, unless stated otherwise, all the energy scales will be measured in units of half bandwidth W.

A. Spectral function

In Fig. 1 we show the evolution of the spectral function,

$$A_d(\omega) = -\frac{1}{\pi} \mathrm{Im}[G(\omega^+)], \tag{38}$$

as a function of U and T. Similar results have been obtained previously by other authors [24]. For completeness we show these results here because they illustrate the essential physics (the destruction of quasiparticles) behind violation of the MIR limit and Hartnoll's bound. In Fig. 1(a) we show the spectral function for a weakly correlated system $U = 0.5$. The spectral function is dominated by a broad central peak and a very small smearing of the noninteracting ($U = 0$) band edges at $\omega = \pm 1$. The integrated spectral weight is dominated by the contribution from the central peak and $A_d(0) \simeq 2/\pi$, as in the noninteracting case. At finite temperature, due to particle-hole excitations across the Fermi surface, the spectral weight at the Fermi energy $\omega = 0$ gets transferred to finite frequency but the central peak still remains intact.

As we increase the correlation strength ($U = 1$) side bands develop on either side of the central peak as shown in Fig. 1(b).

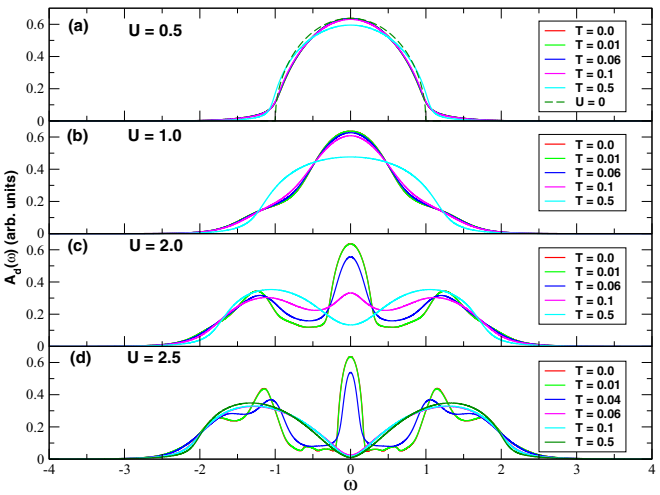

FIG. 1. (Color online) Energy dependent spectral function $A_d(\omega)$ for various values of the interaction strength U and temperature T. Panel (a): weakly correlated regime. (Green) dashed line is the density of states for the noninteracting case. Panel (b): moderately correlated regime. Panels (c) and (d): strongly correlated regime. With increasing U, the integrated spectral weight under central peak (Kondo resonance) gets transferred to high-energy Hubbard bands which corresponds to destruction of quasiparticle states. In these cases, there is a temperature-dependent crossover between strong-coupling regime (Fermi liquid) and local-moment regime (bad metals). All energies and temperatures are measured in units of W, the half bandwidth.

The sidebands eventually develop into high-energy Hubbard bands at $\omega = \pm\frac{U}{2}$ as shown in Fig. 1(c) for $U = 2$. The Hubbard bands are well separated from the central peak which arises due to Kondo resonance effects in the effective single impurity Anderson model [19]. The width and height of the Kondo resonance is controlled by the effective Kondo temperature T_K. Since $T_K \sim W \exp(-\Gamma_{\rm eff}/U)$, where $\Gamma_{\rm eff}$ is an effective hybridization strength, the width of the Kondo resonance decreases while its height increases with increasing U as shown in Fig. 1(d) for $U = 2.5$. For very large $U > U_c$ the Kondo resonance gets completely killed and we enter into the Mott insulating state characterized by fully gapped spectral function at the Fermi energy. The numerical value of U_c depends on the numerical technique that one uses and $U_c \simeq 3.3 - 3.4$ for the IPT based impurity solver [24,26].

At finite temperature in the moderately correlated regime like $U = 1.0$ the central peak, despite getting broadened, remains intact even for temperatures as high as $T \sim W$. The sidebands thermally broaden out. For the strongly correlated regime of $U = 2$ and $U = 2.5$ the central peak (quasiparticle peak) as well as the integrated spectral weight under it decrease with increasing temperature and eventually the central peak gets completely destroyed for temperatures $T \gg T_K$. This corresponds to the finite temperature crossover from the *strong-coupling regime* into the *local moment regime* of the effective Anderson impurity model. The crossover region becomes increasingly sharp as evident in Fig. 1(d), which corresponds to the fragile nature of the quasiparticle state.

B. Quasiparticle weight

In Fig. 2 we show the continuous decrease of the quasiparticle renormalization factor Z with increasing U. This also tracks the continuous destruction of coherent quasiparticle states. Comparison of Z against results from numerical renormalization-group (NRG) based calculations by Bulla [26] validates the qualitative correctness of the IPT based approach though Z begins to differ by 50% in the strong correlation regime ($U = 2.5$). We also note that for $U = 2.5$, $Z > 0.2$ and so in some sense for that regime the system is not extremely correlated. Yet we will see that even in this regime Hartnoll's bound is violated. For comparison, in the doped Hubbard model on the square lattice (with $U = 16t = 3.5W$ at 15% doping $n = 0.85$) DMFT gives $Z \simeq 0.2$ [4].

C. Charge compressibility

In Fig. 2 we also show the evolution of the zero-temperature charge compressibility κ_e as a function of correlation strength U. The charge compressibility continuously goes to zero with increasing U. As mentioned earlier, $1/\kappa_e$ can be thought of as the energy required to add/remove an electron to/from the systems. Hence it gets increasingly harder to add or remove an electron into the system as we increase U, i.e., the system increasingly becomes incompressible and finally at $U = U_c$ the system becomes completely incompressible. Note that at $U = 0$, $\kappa_e = N_0(E_F) = 2/\pi$, as it should be. A similar decrease in charge compressibility with increasing U was observed in exact diagonalization calculations for the Hubbard model on the triangular lattice at half filling [37].

In Fig. 3 we show the temperature dependence of the charge compressibility for a range of values of U. In the noninteracting case ($U = 0$) we can show that

$$\kappa_e(T) = \int_{-\infty}^{+\infty} \left(-\frac{\partial n_F(\omega)}{\partial \omega}\right) N_0(\omega). \tag{39}$$

This expression is similar to that for the Pauli spin susceptibility $\chi(T)$, and the associated temperature dependence is shown in Fig. 3 as a dashed line. The steady decrease in the charge compressibility with increasing temperature is largely due to the broadening of the Fermi-Dirac distribution function.

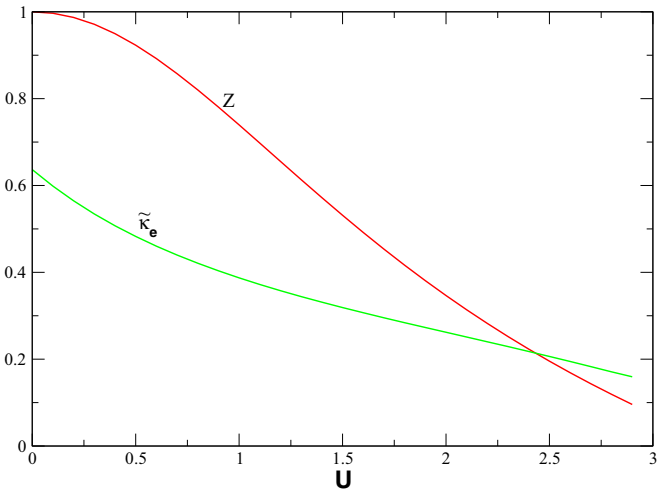

FIG. 2. (Color online) The zero-temperature quasiparticle renormalization factor Z and charge compressibility κ_e as a function of U. The system becomes increasingly incompressible with increasing U and the quasiparticle weight Z smoothly decreases, as the transition to the Mott insulator is approached at $U_c \simeq 3.4$ [26]. U is measured in units of W.

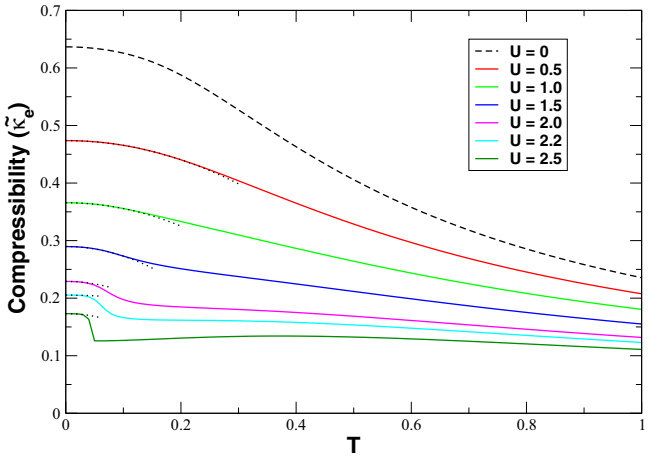

FIG. 3. (Color online) Temperature dependence of the charge compressibility κ_e for various correlation strengths U. The dashed line is the noninteracting ($U = 0$) case calculated using Eq. (39) and dotted lines are quadratic fits to the Fermi-liquid form Eq. (43). The apparent kinklike behavior for $U = 2.5$ is due to the sharp crossover between the Fermi liquid and the bad metal (local moments fixed point). Both T and U are measured in units of W.

Using standard integral expressions involving the Fermi function [38],

$$\int_{-\infty}^{+\infty} H(\epsilon) n_F(\epsilon) d\epsilon = \int_{-\infty}^{\mu} H(\epsilon) d\epsilon + \frac{\pi^2}{6}(k_B T)^2 H'(\mu) + \cdots, \quad (40)$$

the expression for the charge compressibility in Eq. (39) reduces to

$$\kappa_e(T) = N_0(\mu) + \frac{\pi^2}{6}(k_B T)^2 \frac{d^2 N_0(\omega)}{d\omega^2}\bigg|_{\omega=\mu} + \cdots. \quad (41)$$

For the Bethe lattice this reduces to

$$\kappa_e(T) \simeq \frac{2}{\pi W}\left[1 - \frac{\pi^2}{6}\left(\frac{k_B T}{W}\right)^2 + \cdots\right]. \quad (42)$$

In the interacting case we expect in the Fermi-liquid state

$$\kappa_e(T) \simeq \kappa_e(0)\left[1 - \frac{\delta}{Z^2}\left(\frac{k_B T}{W}\right)^2 + \cdots\right], \quad (43)$$

with $\delta \sim 1$. So, because of the thermal broadening effects, just as in the case of the spin susceptibility, the charge compressibility in the Fermi-liquid state will decrease quadratically in temperature at low temperatures. This quadratic dependence is shown in Fig. 3 as dotted lines that have been fitted to the low-temperature behavior. This explains the rapid decrease of the charge compressibility at low temperatures in the coherent Fermi-liquid state, because the temperature scale for the decrease is that of the coherence temperature which close to the Mott transition becomes very small [2,19].

D. Resistivity

In Fig. 4 we show the temperature dependence of the resistivity $\rho(T)$ scaled by the Mott-Ioffe-Regel limit, $\rho_{\rm MIR} = ha/e^2$, for various correlation strengths U. In the weakly correlated regime ($U = 0.5$) the resistivity is well within the Mott-Ioffe-Regel limit in the entire temperature range up to W. Hence, the transport can be characterized by weak scattering of coherent quasiparticle states. At very low temperatures ($T < T_K \ll W$) the resistivity is proportional to T^2 as expected in the coherent Fermi-liquid regime. The T^2 behavior is due to the fact that in the Fermi-liquid regime the imaginary part of the self-energy, or equivalently the inverse of quasiparticle lifetime (τ_{qp}^{-1}), is proportional to T^2 (or ω^2 at $T = 0$). At high temperatures ($T \gg T_K$), the resistivity is roughly linear in T and this corresponds to the incoherent (bad metal) regime of transport [3].

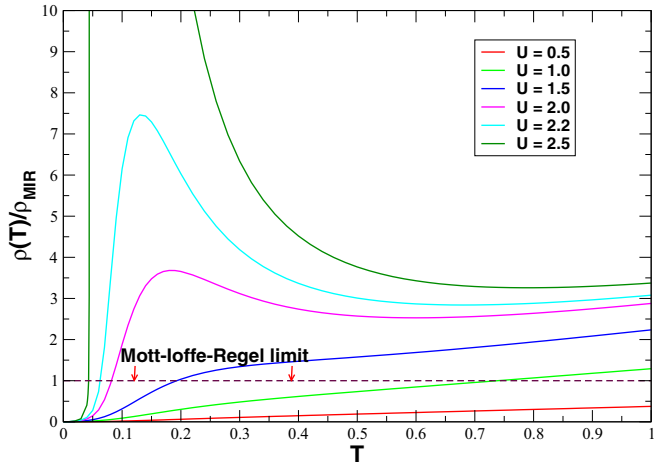

FIG. 4. (Color online) Resistivity shows violation of the Mott-Ioffe-Regel limit ($\rho_{\rm MIR} = ha/e^2$) with increasing U. This is consistent with the picture that transport becomes increasingly incoherent with increasing correlation effects. Both T and U are measured in units of W.

As we increase U, the resistivity smoothly crosses the Mott-Ioffe-Regel limit and in the strongly correlated regime ($U = 2.0$ and above) the resistivity far exceeds the MIR limit. This is due to the sharp crossover from the strong-coupling (Fermi-liquid) regime to the local moment (bad metal) regime in the strong correlation regime and is consistent with the picture of fragile quasiparticles states in the strong correlation regime.

In elemental crystals one can distinguish metals and insulators by the temperature dependence of the resistivity. It is monotonically increasing (decreasing) with increasing temperature for metals (insulators). However, this criteria is unreliable for strongly correlated electron materials. For example, a nonmonotonic temperature dependence of the resistivity in a bad metal is seen experimentally in a number of organic charge salts. [See for example the inset of Fig. 2(a) of Ref. [39].] Thus it is important to note that even though the derivative $d\rho(T)/dT$ changes sign for some curves in Fig. 4 there is no metal-insulator transition, i.e., all the curves are for the metallic phase. This is evident from the finite temperature spectral function, $A_d(\omega)$ at $\omega = 0$, and the nonzero charge compressibility κ_e.

It should also be stressed that for the given choice of U we are still far away from the Mott transition at $U_c \simeq 3.4$. This is also evident from the relatively large quasiparticle weight $Z \sim 0.2$ even for $U = 2.5$ where the MIR limit is violated by a factor of 100. So, the transport in this bad metal phase is incoherent in nature.

E. Diffusivity

Finally, using the Nernst-Einstein relation we calculate the charge diffusivity. In Fig. 5 we show the scaled diffusivity, $D(T)/D_H^*$, as a function of temperature (T) for various correlation strengths (U). In the weakly correlated regime ($U = 0.5$) and moderately correlated regime ($U = 1.0$ and $U = 1.5$) the scaled diffusivity satisfies Hartnoll's bound. However in the strongly correlated regime, $U = 2.0$ and above, the scaled diffusivity shows violation of Hartnoll's bound in the low-temperature region. But at high temperatures $T \gg T_K$ the scaled diffusivity satisfies Hartnoll's bound. It is important to mention that the kinklike behavior at around $T \sim 0.05$ for $U = 2.5$ is closely related to the sharp crossover between the Fermi-liquid fixed point and the local moment fixed point in the effective single impurity Anderson model. As we can see from Fig. 5 the violation of Hartnoll's bound in strongly correlated systems is in the crossover region between coherent (Fermi-liquid) regime and incoherent (local-moment) regime. The magnitude of violation increases with increasing U due to increased sharpness in crossover region. In the

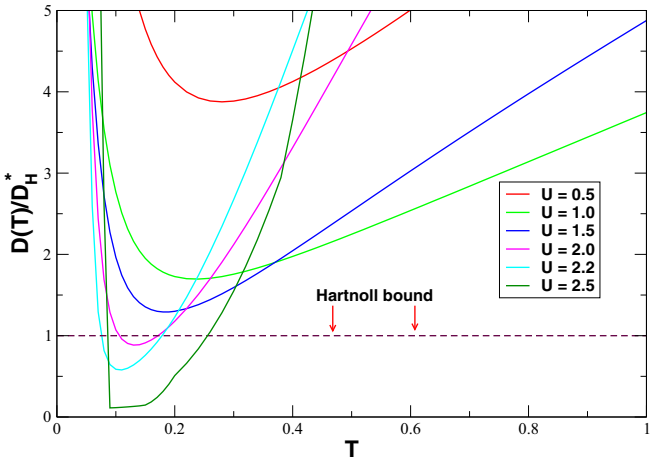

FIG. 5. (Color online) Scaled diffusivity shows violation of Hartnoll's bound in the strongly correlated incoherent regime of transport in the low-temperature region. However, in strongly correlated systems at large temperatures ($T \gg T_K$) and for weakly correlated systems at all temperatures the bound is respected. Kinklike behavior for $U = 2.5$ is due to sharp crossover between the Fermi-liquid and the local-moment regimes. Both T and U are measured in units of W.

high-temperature region, where the resistivity is roughly linear in T, the scaled diffusivity is well above the Hartnoll's bound, provided one uses the renormalized Fermi velocity.

Finally, we compare the charge diffusivity to the quantum limit of the spin-diffusion constant, $D_s \simeq 1.3\hbar/m$, experimentally observed [14] and theoretically calculated [16] in the degenerate Fermi gas in the unitary limit. In Fig. 6 we show the scaled diffusivity, $D(T)/D_A^*$, as a function of temperature for various U. The scaled diffusivity also violates

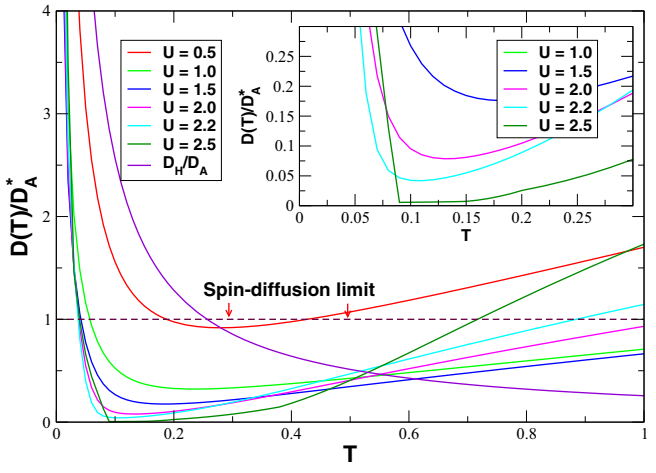

FIG. 6. (Color online) Scaled diffusion constant for charge transport also violates quantum limit for spin-diffusion constant in the incoherent regime of transport. Inset: Detailed plot near the origin shows small yet nonvanishing scaled diffusivity for $U = 2.5$. D_H/D_A traces out the temperature dependence, $1/3\alpha k_B T$, of the Hartnoll bound showing how for $T < 0.3$ it is larger than the proposed bound on the spin-diffusion constant for cold atoms. Both T and U are measured in units of W.

the quantum limit of spin-diffusion constant, $D_s \simeq 1.3\hbar/m$. The violation is severe in the strongly correlated regime. All the temperature dependence is ultimately due to inherent temperature dependence of the self-energy $\Sigma(\omega)$.

It is important to mention that spin diffusion in charge neutral systems like the degenerate Fermi gas in the unitary limit has no clear relation to charge diffusion in electron liquids. In charged systems there are dynamical screening effects while such screening effects are not present in neutral atomic gases such as the strongly interacting degenerate Fermi gas at Feshbach resonance. Most interestingly in a Mott insulator the charge-diffusion constant is zero while the spin-diffusion constant is finite. The differences illustrate different mechanisms for charge and spin transport in strongly correlated systems and one should not necessarily expect any simple relationship between the spin- and charge-diffusion constants.

For a degenerate noninteracting Fermi gas in three dimensions the charge-diffusion constant is given by $D = \frac{1}{3}\frac{\hbar}{m}k_F\ell$, where k_F is the Fermi wave vector and ℓ is the mean free path. In the weak scattering limit $k_F\ell \gg 1$ and $D \gg \frac{1}{3}\frac{\hbar}{m}$. So, just like the upper limit (MIR) of resistivity we can define lower limit for the charge-diffusion constant $D_{\rm lim} = \frac{1}{3}\frac{\hbar}{m}$. In the weakly interacting quasiparticle regime of transport the limit will be renormalized to $D^*_{\rm lim} = \frac{1}{3}\frac{\hbar}{m^*}$. The quantum spin-diffusion limit in degenerate Fermi gas will roughly correspond to $k_F\ell \sim 4$ for charge diffusion in a condensed-matter system and the diffusion will correspond to transport through coherent quasiparticle states.

V. CONCLUSIONS

We have studied the conductivity, charge compressibility, and charge diffusivity in a single band Hubbard model using single-site dynamical mean-field theory. The calculated resistivity far exceeds the MIR limit in the strong correlation regime. The transport in the weakly correlated region can be characterized by diffusive scattering of coherent quasiparticle states but in the strongly correlated bad metal state the transport is incoherent. The charge compressibility decreases with increasing U which corresponds to the fact that in the correlated regime, the energy cost to create a charge fluctuation increases with increasing U. Then using the Nernst-Einstein relation we calculated the charge diffusivity in the system. In the weakly and moderately correlated systems the scaled diffusivity respects Hartnoll's bound at all temperatures. However, in the strongly correlated systems the bound is violated in the crossover region between the coherent Fermi-liquid regime and incoherent local moment regime. In the high-temperature region ($T \gg T_K$), particularly in the region where resistivity is roughly linear in T, the bound is found to be respected for all interaction strengths.

We also compared the calculated charge diffusivity against the quantum limit of spin diffusion observed in the degenerate Fermi gas in the unitary limit. The calculated diffusivity strongly violates the quantum limit of spin diffusion in the incoherent regime. So, within the single-site DMFT approximation we do not observe any quantum limit to charge diffusion in the strongly correlated incoherent regime.

Hartnoll's proposed bound is based on the AdS/CFT correspondence and various conservation laws in fluids.

But within single-site DMFT approximation there is energy conservation but no momentum conservation at a given site. On the other hand, the spatial fluctuations neglected in single-site DMFT can be systematically incorporated through other approximations such as the dynamical cluster approximation (DCA) [40,41]. In DCA the momentum is conserved within the cluster, the bath and at the boundary between the cluster and the bath. One might also consider how vertex corrections could modify the results. For a doped Hubbard model it was found in a four-site DCA calculation that the vertex corrections to the optical conductivity were not significant, except very close to the Mott insulator [42]. A study of the doped two-dimensional Hubbard model using a two-particle self-consistent approach found that vertex corrections altered the calculated resistivity by less than a factor of 2 [43].

As has been pointed out [44] the interacting many electron system in strongly correlated materials so far has no gravity description and hence the strongly coupled gauge theory has no dual description. To be more precise, holographic quantum systems associated with known gravity descriptions have no direct relation with strongly correlated electron systems. Furthermore, the AdS/CFT correspondence only describes conformally invariant field theories and except for one-dimensional systems at a quantum critical point, it is not clear that strongly correlated electron systems are conformally invariant [13].

ACKNOWLEDGMENTS

We acknowledge helpful discussions with X. Deng, J. K. Freericks, S. Hartnoll, H. R. Krishnamurthy, B. J. Powell, T. V. Ramakrishnan, D. Tanaskovic, A. Taraphder, N. Vidhyadhiraja, and J. Vucicevic. This work was supported by a Discovery Project grant from Australian Research Council.

APPENDIX: DERIVATION OF THE NERNST-EINSTEIN RELATION

Fick's law for diffusion is given by

$$\mathbf{j}_m(\mathbf{r}) = -D(T)\nabla n(\mathbf{r}), \tag{A1}$$

where $D(T)$ is the diffusion constant, $\mathbf{j}_m(\mathbf{r})$ is the *mass current*, and $n(\mathbf{r})$ is the *local particle number*. On the other hand, Ohm's law for electrical conductivity is given by

$$\mathbf{j}_e(\mathbf{r}) = \sigma(T)\mathbf{E}(\mathbf{r}), \tag{A2}$$

where $\sigma(T)$ is the electrical conductivity, $\mathbf{j}_e(\mathbf{r})$ is the *electric current*, and $\mathbf{E}(\mathbf{r})$ is the external electric field. We have

$$\mathbf{j}_e(\mathbf{r}) = e\mathbf{j}_m(\mathbf{r}) = -eD(T)\frac{\partial n}{\partial \mu}\nabla\mu(\mathbf{r}), \tag{A3}$$

where $\mu(\mathbf{r}) = \mu_0 + e\phi(\mathbf{r})$ is the chemical potential in the presence of external field and μ_0 is that in the absence of external field and $\phi(\mathbf{r})$ is the electric potential. Then

$$\nabla\mu(\mathbf{r}) = e\nabla\phi(\mathbf{r}) = -e\mathbf{E}(\mathbf{r}). \tag{A4}$$

Combining Eqs. (A3) and (A4) gives

$$\mathbf{j}_e(\mathbf{r}) = e^2\frac{\partial n}{\partial \mu}D(T)\mathbf{E}(\mathbf{r}). \tag{A5}$$

Comparing this with Ohm's law in Eq. (A2) we finally get

$$\sigma(T) = e^2\frac{\partial n}{\partial \mu}D(T). \tag{A6}$$

[1] N. E. Hussey, K. Takenaka, and H. Takagi, Philos. Mag. **84**, 2847 (2004).
[2] J. Merino and R. H. McKenzie, Phys. Rev. B **61**, 7996 (2000).
[3] X. Deng, J. Mravlje, R. Zitko, M. Ferrero, G. Kotliar, and A. Georges, Phys. Rev. Lett. **110**, 086401 (2013).
[4] W. Xu, K. Haule, and G. Kotliar, Phys. Rev. Lett. **111**, 036401 (2013).
[5] S. Sachdev and M. Müller, J. Phys.: Condens. Matter **21**, 164216 (2009).
[6] T. Faulkner, N. Iqbal, H. Liu, J. McGreevy, and D. Vegh, Science **329**, 1043 (2010).
[7] J. M. Maldacena, Adv. Theor. Math. Phys. **2**, 231 (1998).
[8] P. K. Kovtun, D. T. Son, and A. O. Starinets, Phys. Rev. Lett. **94**, 111601 (2005).
[9] E. Shuryak, Prog. Part. Nucl. Phys. **53**, 273 (2004).
[10] C. Cao, E. Elliott, J. Joseph, H. Wu, J. Petricka, T. Schäfer, and J. E. Thomas, Science **331**, 58 (2011).
[11] T. Schäfer, Ann. Rev. Nucl. Part. Sci. **64**, 125 (2014).
[12] S. A. Hartnoll, Nat. Phys. **11**, 54 (2014).
[13] P. W. Anderson, Phys. Today **66**(4), 9 (2013).
[14] A. Sommer, M. Ku, G. Raoti, and M. W. Zwierlein, Nature (London) **472**, 201 (2011).
[15] A. B. Bardon *et al.*, Science **344**, 722 (2014).
[16] T. Enss and R. Haussmann, Phys. Rev. Lett. **109**, 195303 (2012).
[17] M. Koschorreck, D. Pertot, E. Vogt, and M. Köhl, Nat. Phys. **9**, 405 (2013).
[18] W. Metzner and D. Vollhardt, Phys. Rev. Lett. **62**, 324 (1989).
[19] A. Georges, G. Kotliar, W. Krauth, and M. J. Rozenberg, Rev. Mod. Phys. **68**, 13 (1996).
[20] P. Limelette, P. Wzietek, S. Florens, A. Georges, T. A. Costi, C. Pasquier, D. Jerome, C. Meziere, and P. Batail, Phys. Rev. Lett. **91**, 016401 (2003).
[21] J. Merino, M. Dumm, N. Drichko, M. Dressel, and R. H. McKenzie, Phys. Rev. Lett. **100**, 086404 (2008).
[22] B. J. Powell and R. H. McKenzie, Rep. Prog. Phys. **74**, 056501 (2011).
[23] G. Kotliar, S. Y. Savrasov, K. Haule, V. S. Oudovenko, O. Parcollet, and C. A. Marianetti, Rev. Mod. Phys. **78**, 865 (2006).
[24] X. Y. Zhang, M. J. Rozenberg, and G. Kotliar, Phys. Rev. Lett. **70**, 1666 (1993).
[25] H. Kajueter and G. Kotliar, Phys. Rev. Lett. **77**, 131 (1996).
[26] R. Bulla, Phys. Rev. Lett. **83**, 136 (1999).
[27] H. Terletska, J. Vučičević, D. Tanasković, and V. Dobrosavljević, Phys. Rev. Lett. **107**, 026401 (2011).
[28] L.-F. Arsenault, P. Sémon, and A.-M. S. Tremblay, Phys. Rev. B **86**, 085133 (2012).
[29] E. Economou, *Green's Functions in Quantum Physics* (Springer, Berlin, Heidelberg, 2010).

[30] A. Khurana, Phys. Rev. Lett. **64**, 1990 (1990).
[31] T. Pruschke, D. L. Cox, and M. Jarrell, Phys. Rev. B **47**, 3553 (1993).
[32] W. Chung and J. K. Freericks, Phys. Rev. B **57**, 11955 (1998).
[33] A. Chattopadhyay, A. J. Millis, and S. Das Sarma, Phys. Rev. B **61**, 10738 (2000).
[34] L.-F. Arsenault and A.-M. S. Tremblay, Phys. Rev. B **88**, 205109 (2013).
[35] J. M. Luttinger, Phys. Rev. **119**, 1153 (1960).
[36] T. Hotta and S. Fujimoto, Phys. Rev. B **54**, 5381 (1996).
[37] J. Kokalj and R. H. McKenzie, Phys. Rev. Lett. **110**, 206402 (2013).
[38] N. Ashcroft and N. Mermin, *Solid State Physics* (Saunders, Philadelphia, 1976).
[39] Y. Kurosaki, Y. Shimizu, K. Miyagawa, K. Kanoda, and G. Saito, Phys. Rev. Lett. **95**, 177001 (2005).
[40] T. Maier, M. Jarrell, T. Pruschke, and M. H. Hettler, Rev. Mod. Phys. **77**, 1027 (2005).
[41] N. Lin, E. Gull, and A. J. Millis, Phys. Rev. B **82**, 045104 (2010).
[42] N. Lin, E. Gull, and A. J. Millis, Phys. Rev. B **80**, 161105 (2009).
[43] D. Bergeron, V. Hankevych, B. Kyung, and A.-M. S. Tremblay, Phys. Rev. B **84**, 085128 (2011).
[44] Hong Liu, Phys. Today **65**(6), 68 (2012).